Dynamic response of the cusp morphology to the solar wind: A case study during passage of the solar wind plasma cloud on February 21, 1994

M. Yamauchi,[1] H. Nilsson,[1] L. Eliasson,[1] O. Norberg,[1] M. Boehm,[2] J. H. Clemmons,[3] R. P. Lepping,[3] L. Blomberg,[4] S.-I. Ohtani,[5] T. Yamamoto,[6] T. Mukai,[6] T. Terasawa,[7] and S. Kokubun[8]

(accepted manuscript)
J. Geophys. Res., 101, 24675-24687, 1996 (copyright © 1994 by the American Geophysical Union)
https://doi.org/10.1029/96JA01873

Abstract. On February 21, 1994, both Geotail and IMP 8 satellites detected an interplanetary plasma cloud with intense interplanetary magnetic field (IMF > 50 nT) and high dynamic pressure (> 50 nPa). During this interval the Freja satellite detected intense cusp-like plasma injections in four out of six dayside traversals. The first two traversals are carefully studied. During the first traversal the overall morphology of the ion injection is characterized by a "multiple-injection" signature over a wide magnetic local time (MLT) range, whereas it is characterized by a "single-injection" signature with narrow injection region at 8 MLT in the second traversal. The solar wind conditions were also quite different between these two periods: while both dynamic and magnetic pressures stayed high during entire period, the dynamic beta was much higher during the first Freja traversal than during the second traversal. Between these two traversals, the cusp plasma injection is detected by the Søndre Strømfjord radar. The radar signature of the plasma injection is identified using the satellite particle data when the satellite and the radar were conjugate (the satellite's footprint was in the radar's field of view.) The cusp position and dynamics observed by the Søndre Strømfjord radar again show a very good correlation to the solar wind condition, especially to the dynamic pressure. The result indicates the following. (1) During southward IMF the cusp morphology differs for conditions of high or low solar wind dynamic pressure. High

[1]Swedish Institute of Space Physics, Kiruna.
[2]Jet Propulsion Laboratory, Pasadena, California.
[3]NASA/Goddard Space Flight Center, Greenbelt, Maryland.
[4]Institute of Plasma Physics, Royal Institute of Technology, Stockholm, Sweden.
[5]Johns Hopkins University Applied Physics Laboratory, Laurel, Maryland.
[6]Institute of Space and Astronautical Science, Sagamihara, Japan.
[7]Department of Earth and Planetary Physics, Tokyo University, Tokyo, Japan.
[8]Solar Terrestrial Environment Laboratory, Nagoya University, Toyokawa, Aichi 442, Japan

dynamic pressure widens the cusp (with multiple injections), whereas high magnetic pressure narrows it (with single injection). The effect of the IMF on the cusp locations and morphology becomes dominant only when the dynamic pressure is not very high. (2) Such a morphological difference reflects dynamic pressure more than dynamic beta during southward IMF at least during times of high solar wind dynamic pressure. (3) The cusp morphology responds very quickly to the changes in the solar wind conditions.

1. Introduction

It has long been known that the ionospheric cusp morphology and its position are affected by the interplanetary magnetic field (IMF) conditions or by the interplanetary electric field (a product of IMF and the solar wind velocity (V_{SW})) conditions. Many studies have been dedicated to this subject for both north-south (B_Z) and dawn-dusk (B_Y) components [e.g., *Friis-Christensen and Wilhjelm,* 1975; *McDiarmid et al.,* 1979; *Clauer and Banks,* 1986; *Newell and Meng*, 1987; *Elphinstone et al.*, 1990; *Maynard et al.*, 1991; *Woch and Lundin*, 1992a; *Yamauchi and Lundin*, 1994]. However, the IMF (or electric field) is not the only factor that controls the cusp morphology and its position. For example, Viking and Freja observations [*Yamauchi and Lundin*, 1994; *Norberg et al.*, 1994] show that the overall cusp morphology is sometimes characterized by a "single-injection" and sometimes by "multiple injections" for arbitrary IMF directions. In most past studies of the cusp, both observational theoretical, only the single-injection has been considered a "typical southward-IMF type" cusp [e.g., *Reiff et al.*, 1977, *Burch et al.*, 1982]. However, in reality, multiple injections are often observed in the cusp as well as in the dayside low-latitude boundary layer (LLBL) [*Carlson and Torbert*, 1980; *Woch and Lundin*, 1992b; *Clemmons et al.*, 1995], and they appear as frequent as the single-injection in the cusp during southward IMF [*Yamauchi and Lundin*, 1994; *Norberg et al.*, 1994]. Therefore parameters other than IMF must play substantial roles in making such a difference.

One obvious factor is the solar wind dynamic pressure (SWDP) because it is known to control local plasma injection events across the magnetopause [*Lemaire*, 1977; *Woch and Lundin*, 1992b]. *Newell and Meng* [1994] showed that statistical sizes of the cusp and the dayside LLBL are strongly affected by the SWDP. This result indicates SWDP control of the cusp morphology because multiple injections are expected to widen the cusp from its "basic" width for a single-injection (the width is roughly multiplied by the number of injections, as is seen in Plate 1 of *Yamauchi et al.* [1995].) Sandholt and his coworkers used a case study to also show that the SWDP controls the dayside aurora activity with short response time [e.g., *Sandholt et al.*, 1994, and references therein]. Under this background, we raise the following questions:

1. How does the morphology of the low-altitude cusp depend on the SWDP?
2. What are the relative contributions of the IMF and the SWDP to the control

of the morphology and location of the low-altitude cusp?

To investigate the above questions by a case study, we need the following observational conditions: (*1*) The values of both the IMF and the SWDP are high enough that their influences overweigh any other possible factors such as seasonal differences. (The seasonal effect is fairly large in the cusp region [e.g., *Yamauchi and Araki*, 1989], and we may not rule out the possibility that the cusp morphology is affected by the solar zenith angle.) (*2*) The cusp is continuously monitored from the ground. This condition is necessary because the response time of the cusp to SWDP changes is unknown. (*3*) The cusp is simultaneously observed from the ground and by satellites. This condition allows us to identify the ground signature of the cusp through the concurrent satellite signatures. (*4*) The IMF and SWDP behave in a way which allows us to separate their relative influence on the cusp morphology.

Recently, we performed a 24-day campaign (April 1993, February 1994, and May-June 1994) consisting of conjugate observations of the cusp region by the Freja satellite and the Søndre Strømfjord incoherent scatter radar [*Nilsson et al.*, 1996]. This campaign happened to include an ideal day (February 21, 1994) that satisfied all the above conditions (*1-4*). Figure 1 shows the solar wind parameters on that day as measured by Geotail and IMP 8 satellites which were located as is shown in Figure 2. At around 0900 UT, both Geotail and IMP 8 detected a historically large interplanetary plasma cloud (most likely due to a coronal mass ejection) with an extremely intense IMF (peak value ≈ 70 nT) and a large SWDP (peak value > 100 nPa). After the initial increase of both the IMF and the SWDP, they varied very dynamically and nearly independently of each other (conditions *1* and *4*). Meanwhile, the velocity is nearly constant; that is, the variation of the interplanetary electric field was nearly the same as that of the IMF, so that it is only necessary to compare with the IMF and the SWDP. Figure 1 includes the interplanetary electric field for reference. Note that the IMP 8 magnetometer saturates for fields larger than 49 nT, causing the data gap at 1358-1512 UT, and that the Geotail particle detector sometimes saturates too as is indicated in Figure 1 (it is not designed to measure such a high-density cloud.)

This interplanetary cloud immediately caused a strong sudden commencement, a large geomagnetic storm, and large substorms afterward. A +38 nT initial jump of *Dst* at 0900-1000 UT succeeded the main phase negative bay starting at 1400 UT reaching -144 nT at 0100-0200 UT next day; the *Kp* was 7^+ for 0900-1800 UT [e.g., *Petrinec et al.*, 1995; *Araki et al.*, 1995]. The extremely high activity continued during the entire period of radar operation (1320-1540 UT). Two Freja traversals (orbits 6651, 6652) were within the radar's field of view. Freja also traversed the dayside auroral region during the four subsequent orbits: two with the cusp signatures (orbits 6653, 6656) and two without the cusp or LLBL signatures (orbits 6654, 6655). During the first satellite-radar conjunction (orbit 6651: 1328 UT) the cusp particle injection is simultaneously observed by the radar and the satellite, and hence the radar

signature of the plasma injection is clearly defined. With this identification the radar data show the dynamics of the cusp morphology in response to the changes in IMF/SWDP conditions during the 2 hours of observation.

2. Satellite observation

Figures 3 and 4 show ion and electron spectrogram of the two consecutive Freja traversals (orbits 6651 and 6652) during the radar operation. The satellite-radar conjunctions occurred at 1328 UT (orbit 6651) and at 1521 UT (orbit 6652), which are nearly 2 hours apart. Descriptions of the Freja mission and instruments are found in *Freja special issue* (*Space Sci. Rev.*, *70*, 405-602, 1994). The satellite observed intense injections of a few keV protons and uniform electron precipitation in a very wide region (7-11 magnetic local time (MLT)) during the first traversal (orbit 6651) and in a narrower region (7-9 MLT) during the next traversal (orbit 6652). The intensity of these proton injections is higher than that in the ordinary cusp proper by a factor of 3-5. The electron precipitation in this region is rather uniform without the spike-like keV acceleration signatures often found in the LLBL. All these features indicate that the region is most likely the cusp rather than the LLBL except that the peak energy of the electron flux is a little higher (300 eV) than in the ordinary cusp proper (50-100 eV). The DMSP satellite which passed through near local noon at around 1400 UT also shows the same features with extremely intense, uniform, and widely extended injection (P. Newell, privation communication, 1996), confirming that the 300-eV electron energy does not prevent identifying this region as the cusp. The 300-eV peak of the electron energy flux may be attributed to high solar wind velocity (V_{SW} = 800 km/s, which means more thermalization after bow shock [*Newell and Meng*, 1994]) and/or a large-scale field-aligned potential structure due to high influx of protons. Thus, although there is some ambiguity in distinguishing between the cusp and the LLBL for this "extremely" high SWDP case, we here identify it the cusp. By doing so, we do not lose the primary purpose of this paper because the extremely high intensity anyway indicates that these injections must have come directly from dayside magnetosheath and not from dawn or dusk franks. The cusp was located extremely far dawnward (especially for orbit 6652), which is consistent with the large negative IMF B_Y during these traversals.

The morphologies of the ion injections differ between orbit 6651 and orbit 6652. The former (orbit 6651) consists of several independent injections (so-called multiple-injections [*Yamauchi and Lundin*, 1994; *Norberg et al.*, 1994]). Individual impact regions are widely scattered at 8.2, 8.8, 9.1, 9.5, 10.1, and 10.8 MLT. The latter (orbit 6652) is characterized by a single large-scale dispersion (so-called single-injection) from 1511:40 UT to 1516:10 UT. Freja electric field and magnetic field data show consistent characteristics (not shown here): many mesoscale (few minutes) variations are dominating in orbit 6651, whereas one systematic large-scale variation is seen in orbit 6652. Multiple injections are

seen also in orbits 6653 and 6656 (not shown here), but they are not as wide or intense as orbit 6651.

Orbit 6652 is the only Freja traversal with single-injection type cusp on February 21, 1994. The field measurement of this orbit is peculiar with extremely strong sunward and antisunward convection before and after 1511:20 UT. Figure 5 shows the Freja observation of the electric field and magnetic field for orbit 6652. The baseline for the electric field is somewhat shifted to minus value as is indicated in Figure 5. A large tailward ΔB is detected during 1509:40-1511:20 UT between the upward region 2 field-aligned current and downward region 1 field-aligned current at 7 MLT. This indicates a strong sunward convection and shows that this region cannot be identified as the cusp. According to direct measurement by electric field instruments, it is as strong as 50 mV/m, corresponding to a convection speed of 1 km/s. The particle measurements indicate that the sunward convection region (much less intense proton injection) is consistent with an interpretation as being the LLBL (or the LLBL/stagnation region (SR) of *Woch and Lundin* [1993]) rather than the enhanced plasma sheet, although the convection direction indicates opposite. We do not further identify the region because this is an extremely disturbed period. After 1511:40 UT, when the single-injection of the cusp particle started, we see a steady antisunward convection (up to > 80 mV/m), which is consistent with the radar observation of the ion flow (1-2 km/s). The strong electric field indicates at least 150 kV potential drop along the single-injection part of the Freja trajectory, which is the largest potential drop ever observed in the dayside during more than 2 years of Freja operation. All of these data (particle, electric field, and magnetic field) indicate a widening of the polar cap.

3. Radar Observation

The radar observations provide dynamics of the cusp morphology in response to the solar wind variation if we can identify the radar signature of the cusp. Although the incoherent radar signature of the cusp has been studied [e.g., *Watermann et al.*, 1994], it is not necessarily the same for different cusp types [*Nilsson et al.*, 1996]. It is necessary to compare the radar and satellite data for each case because there are not enough statistics for each type. In the present case, we compared the Søndre Strømfjord incoherent scatter radar data with the Freja satellite data near the radar-satellite conjunction for orbits 6651 and 6652, and identified the radar signature of the cusp for these particular orbits. The signature is used to monitor the cusp during the period between these two orbits. The identified signature is not very different from the other radar signatures of the cusp. We see a solid region of electron temperature (T_e) enhancement in the cusp. In addition, we see an electron density (N_e) enhancement.

The radar measurements of the February 21, 1994 event are shown in Figure 6. The measurement mode is described by *Nilsson et al.* [1996]. For exact comparisons, Figure 1 is expanded during 1300-1430 UT in Figure 7. The

magnetic and dynamic pressures are also plotted. In the first three scans (1324-1333 UT), one can see a very strong T_e enhancement in the entire field of view except its equatorward-most part (left in each panel). This T_e enhancement weakened in the following three scans 4-6 (1335-1343 UT), then resumed in the subsequent several scans 7-12 (1344-1404 UT). Proceeding to the strong T_e enhancements, we detected N_e enhancements in the *F* region, moderate ion temperature (T_i) enhancements, and then a mostly poleward ion convection.

At the end of this intense precipitation event the particle precipitation became energetic (a solid region of ionization well below 200 km altitude), and its location began to move equatorward at around 1403 UT. Subsequently, a deep trough started at around 1410 UT, and the T_e enhancement disappeared from the radar's field of view at 1415 UT. Magnetosheath particle injection (appeared as T_e enhancement) did not reappear for more than 1 hour. At 1526 UT a cold electron density enhancement was observed together with some enhancement of T_e. This is probably caused by the precipitation equatorward of the radar. The ion temperature, which was moderate in the beginning, increased drastically at scan 6, coincident with an eastward turning of the poleward drift. Then, after scan 8, T_i kept moderate until the large-scale convection turned westward at around 1410 UT.

The T_e enhancement is usually used to diagnose the cusp proper instead of the N_e enhancement because the electron temperature rises faster in response to soft precipitation [e.g., *Roble and Rees*, 1977], and one does not have a problem with the long lifetime of the *F* region plasma (i.e., N_e enhancement may be just cold plasma blobs.) However, the unusually high characteristic energy of the precipitating cusp electron (see previous section) with the extremely high influx (a factor of 5 more intense than ordinary Freja cusp cases) must give a clear signature in the N_e data below 200 km (precipitating electrons give about one ionization per 35-eV energy of the primary particle, and the higher the energy, the lower the altitude where such an ionization takes place [e.g., *Rees*, 1989].) In fact, both distributions are very similar as is clear by comparing the first row and the second row of Figure 6 as is expected. The higher injection energy than the ordinary cusp electrons also means less T_e enhancement than the ordinary cusp proper. For example, in scan 6 the N_e enhancement is very pronounced in its equatorward portion, suggesting energetic particle precipitation (ionization well below 200 km altitude) after the density trough of scans 4 and 5, whereas we do not see T_e enhancements there as strong as in the usual cusp proper [*Nilsson et al.*, 1996]. Also, one can easily recognize two separated structures in N_e data in the first two scans (1323:32 - 1326:35 UT, 1326:40 - 1329:43 UT), while it is not as clear in the T_e plot. Since T_i is not very enhanced in this scan, the density trough cannot be attributed to enhanced recombination, and the gap in N_e must be a real gap of the electron precipitation.

With these special reasons which apply specifically to this day, we use electron density measurements for studies of the cusp morphology. Plate 1 shows the

overall two-dimensional mapping of N_e deduced from Figure 6. Each scan (about 3 min) in Figure 6 occupies one vertical column of Plate 1, and the two-dimensional ion convection pattern (white arrows) is obtained from each pair of northward and southward scans (see *Nilsson et al.* [1996] for the method). The Freja orbits are superposed on the figure (the lower trajectory is orbit 6651; the upper trajectory is orbit 6652.) The conjunctions are at 1328 UT (orbit 6651) and 1521 UT (orbit 6652). Near the first conjunction, Freja observed isolated weak ion precipitation at 70.0°-70.8° corrected geomagnetic latitude (CGLAT), or about 250 km from the most intense particle precipitation region at 1327 UT. If one extends this extremely active region longitudinally, one finds that it corresponds to the extremely enhanced N_e region of scans 1-3 (1325-1332 UT) poleward of the conjugate point. This corresponds to the cusp identified by the satellite in the previous section.

Since the response time of T_e to the electron precipitation is about a second [*Roble and Rees*, 1977], the azimuthally extended (at least 10.5-11.4 MLT) cusp particle precipitation probably continued until 1332 UT after Freja left this extremely active region at 1327:50 UT (71.3° CGLAT) southward. The positive (increase) dispersion of the ion energy seen there is consistent with the clear equatorward boundary of the N_e enhanced region in scan 2. An azimuthal extension of the weak and isolated ion precipitation region also reaches a faintly enhanced N_e region at around 70° CGLAT. This equatorward event is rather sporadic in the radar. Overall, correspondence between the satellite data and the radar data (N_e) is very good for both the timing and the position of the equatorward injection boundary.

In the next conjunction (orbit 6652), Freja traversed an extremely large “open” region (mantle and the polar cap, see section 2) near local noon before encountering a cleft-like region at 1521:20 UT (13.0 MLT). The radar observed the large-scale flow which is usual observed in the polar cap, and no injection was detected until 1521:20 UT when N_e was enhanced (rather sporadic, and not evident in T_e plot). Thus both the satellite and the radar observations indicate that the cusp was located far equatorward (or dawnward as is seen in the Freja particle data at around 1512 UT) of the radar during that period.

4. Solar Wind Control

The satellite cusp morphology is quite different between orbit 6651 (multiple injections) and orbit 6652 (single-injection). This difference is also seen in the radar data, as strong electron precipitation is present near the Freja conjunction for orbit 6651, while the electron trough is observed over the entire radar field of view for orbit 6652. The solar wind conditions during this period (Figures 1 and 7) are quite different between these two orbits in both SWDP and IMF, suggesting that solar wind conditions are the important factors determining the cusp morphology. From Viking observations, multiple injections are more frequently observed during northward IMF [*Yamauchi and Lundin*, 1994]), and

the IMF direction could be the leading factor in their occurrence. However, the low orbital inclination of Freja allows us to observe the cusp only during southward IMF (97% of Freja cusp observations are during southward IMF), and the control exerted by the IMF direction is not the problem studied in the present case. The question is whether the cusp morphology is controlled primarily by the strength of the IMF. The IMF is steady and extremely dawnward (B_Y = -50 nT) during orbit 6652, whereas it is much less intense in orbit 6651 than in orbit 6652. Since strong IMF B_Y substantially works in the same manner as southward IMF, the intensity of the southward IMF (or B_Y) could be the leading factor to determine the cusp morphology. However, we have a problem with multiple injections at orbit 6653. The extremely strong southward and duskward IMF (B_Z = -15 nT and B_Y = -20 nT) incorrectly predicts a single-injection.

We consider instead the combination of the IMF and the SWDP rather than only the IMF. Both the SWDP and the IMF are much more intense than those of the ordinary solar wind, but the SWDP is exclusively high during the first traversal (multiple injections), whereas the IMF is exclusively strong during the second traversal (single-injection). From this we hypothesize that high SWDP causes the cusp morphology to consist of multiple injections, whereas a single injection is seen when the IMF is exceptionally strong (not simply strong). This idea is consistent with the statistical results by *Newell and Meng* [1994], who showed that high SWDP widens the cusp, and by *Woch and Lundin* [1992b] who showed by using Viking that multiple transient plasma injection in the LLBL depends strongly on the SWDP. The Freja observations of orbits 6651-6656 agrees with the hypothesis: the SWDP was rather small during orbits 6654 and 6655 compared to the other orbits, and coincidentally Freja did not observe the cusp or the LLBL in these two orbits. Since Freja's traversals are longitudinal over the cusp region (because of the low inclination), the absence of the cusp in orbits 6654 and 6655 means that the cusp was located far northward of the Freja traversals; that is, it must have been located poleward of 72° CGLAT at orbit 6654 (69° CGLAT for orbit 6655) no matter where the cusp shifted in longitudinal direction. The IMF alone does not explain this, especially the fact that we saw the cusp at orbit 6656 (at 63.5° CGLAT), whereas we did not see it at orbit 6655 (at 69° CGLAT).

It is sometimes argued that dynamic b (ratio of SWDP to magnetic pressure of the IMF) must be more important than SWDP for plasma injections [e.g., *Matsuura*, 1995], and we need to examine this from the data. To do so, we examined all cusp traversals of Freja during its most intensive operation (October 1992 to June 1995). The result is shown in Figure 8. Among more than 100 clear cusp/cleft traversals during the entire Freja mission, there are only 30 clear cases with complete IMP 8 data, and one cannot draw a firm conclusion. Yet, Figure 8 provides some indication: the single-injection cases are restricted only to low SWDP (< 4 nPa), and the cusp is characterized by multiple injections for high SWDP (> 4.5 nPa), with a single exception of orbit 6652; however, both types of

injections are evenly distributed with respect to dynamic b. Apparently, the dynamic b is not, at least, more important than the SWDP. We also examined the IMF dependence in Figure 8. The cusp is again characterized by multiple injections for strong IMF B_Z (B_Z < -10 nT) or E_Y = - $V_{SW}B_Z$ (E_Y > 5 mV/m). However, this is most likely superficial because high SWDP normally accompanies large $|B_Z|$. Even if we restrict ourselves to $|B_Z|$ < 10 nT, the SWDP control of the cusp morphology is still apparent, whereas the IMF control of the cusp morphology is absent if we restrict ourselves to P < 4 nPa. As *Newell and Meng* [1994] pointed out from DMSP satellite data, the SWDP control of the cusp/LLBL sizes is more prominent than the control by IMF, and Figure 8 (Freja satellite data) agrees with this. The result also indicates that a statistical examination of only the IMF may lead to a false conclusion.

Sandholt et al. [1994] showed that a 50% fluctuation in the solar wind can produce activities in the dayside aurora, suggesting that the multiple injections can be caused by those fluctuations. However, the SWDP fluctuation is seen as often near orbit 6652 ("single") as near orbit 6651 ("multiple"). Furthermore, both SWDP and IMF are more stable near orbit 6656 (multiple) than near orbit 6652 (single) according to 6-s resolution data of Geotail. Therefore solar wind fluctuations on a timescale of several minutes are not the only reason for the multiple injections in the cusp, although they certainly contribute.

The importance of the SWDP is also recognized in the radar data. Since we have two satellites measuring the solar wind conditions (Figure 2), we can linearly interpolate the arrival time of the changes (see the Figure 2 caption). There are three dips of IMF B_Z (southward turning) during the same period. Even taking into consideration the IMF B_Y, we see three dips of southward-dawnward IMF at 1333-1340 UT, 1348-1356 UT, and 1404-1525 UT at Geotail. However, in the radar the electron trough (i.e., equatorward-dawnward expansion of the mantle/polar cap) is observed only twice at 1334-1343 UT and 1410-1526 UT, and these timings and durations surprisingly match the pressure dips observed by Geotail and IMP 8 with a time lag of only a few minutes. Clearly, the cusp observation by the radar is better correlated with the SWDP (or total $|B|$) than the IMF (or interplanetary electric field) direction. Since the electron trough is understood as to be in the polar cap for single-injection-type cusp, this result can also be attributed to the morphological change of the cusp by the SWDP. The satellite observations support this. These observations indicate that although southward IMF is a necessary condition to move the cusp equatorward (as is clear from Figure 8b), the SWDP enhances this trend by changing the cusp morphology.

5. Summary of the Observations

We found the following results about the cusp morphology and location:

1. When a large interplanetary plasma cloud hit the Earth on February 21, 1994, a wider cusp with multiple injections was observed during a period of

relatively high SWDP (orbit 6651), whereas a narrower cusp with single-injection was observed a during period of relatively intense IMF (orbit 6652). This dependence of the cusp morphology on SWDP is also supported by a correlation study (Figure 8). SWDP is more influential on the cusp morphology than the dynamic b, IMF, or interplanetary electric field under high SWDP. Fluctuations of the solar wind on a timescale of a few minutes are not the leading cause for the multiple injections in the present case.

2. The radar observations on February 21, 1994, show that the cusp location (latitude) is well correlated with the variation of the SWDP. The magnitude of IMF B_Z (or $V_{SW}B_Z$) is not as influential as SWDP or total $|B|$ during this particular event. The cusp location (and hence probably its morphology too) changed very quickly in response to the change in SWDP. The cusp (or cleft) was not observed at around 70° CGLAT by Freja (the satellite traversals are azimuthal) when SWDP was low (orbit 6655), whereas it was visible when SWDP was high (orbit 6656).

6. Discussions and Conclusion

The February 21 event is very unusual in both solar wind conditions and the magnetosheath plasma injections to the dayside ionosphere. Both the SWDP and the IMF are extremely strong (not merely strong), the particle fluxes detected by Freja and DMSP (not shown here) are extremely strong, and the characteristic electron energy is higher than in the ordinary cusp (300 eV instead of 50-100 eV). Such a unique observation may not be simply generalized to all the other cusp cases under nominal solar wind conditions. Yet the present result clearly shows that the SWDP plays an important role in the direct magnetosheath particle access to the frontside of the Earth and hence in the formation of the cusp. The multiple injections could be driven by relatively high SWDP. Figure 8 reinforces this point.

Many past studies have shown that the cusp location responds to changes in the IMF direction very quickly [*Clauer and Banks*, 1986; *Knipp et al.*, 1991; *Yamauchi et al.*, 1995] when the SWDP is steady. However, the present result indicates that the SWDP is the primary factor over IMF B_Z to control the cusp morphology, position, and size. One may immediately consider the following explanations: (1) These two effects have not been well separated in the past because strong IMF B_Z normally accompanies strong SWDP. (2) SWDP becomes dominant only when it is extremely strong. The IMF plays the primary role in determining the cusp location for lower SWDP. (3) SWDP determines only the cusp morphology (and hence its size), while the IMF B_Z determines its center position.

The first possibility is probably not the case because past researchers have been aware of this problem. Both the second and the third possibilities, i.e., new explanations, are theoretically feasible under the following consideration. Although the IMF determines the magnetic null point, the extent of the “null

region" in which we can ignore the magnetic field compared to the plasma (dynamic plus thermal) pressure depends directly on the SWDP. According to geomagnetic field models, wide null regions exist at high latitudes [*Stasiewicz*, 1991]. Since the plasma seeks such a null region (or "diffusion region" in the traditional reconnection theory) to gain access to the ionosphere, the size of the plasma injection region should also be dependent on the SWDP.

Finally, we propose a hypothesis that under high SWDP the IMF B_Z controls the center latitude of the cusp, whereas the SWDP controls the morphology and spatial extent of the cusp. This hypothesis is consistent with the observation of strong SWDP effects on the cusp size and location [*Newell and Meng*, 1994]. The hypothesis is also consistent with the SWDP dependence of the impulsive plasma injection events in the LLBL observed by Viking [*Woch and Lundin*, 1992b]. Since most of the past work focuses more on the IMF than on the SWDP, we would like to conclude this paper by emphasizing that the IMF is not the only factor that controls the cusp, and it can even be a secondary driver in certain cases. So is the case for the SWDP: There might be another external or internal parameter that is very important in determining the cusp morphology and its location.

Acknowledgments. The geomagnetic field data are provided by WDC-C2 for geomagnetism at Kyoto University. The IMP 8 plasma data are provided by the space research group at MIT, Cambridge. The Freja project is supported by Swedish National Space Board and German Space Agency. The data from the Søndre Strømfjord incoherent scatter radar is provided by SRI International.

The Editor thanks Patrick T. Newell and J. Woch for their assistance in evaluating this paper.

References

Araki et al., Geomagnetic sudden commencement on February 21, 1994, II, *STEP GBRSC News, 5*, no. 1, 1995.

Burch, J. L., P. H. Reiff, R. A. Heelis, J. D. Winningham, W. B. Hanson, C. Gurgiolo, J. D. Menietti, R. A. Hoffman, and J. N. Barfield, Plasma injection and transport in the midaltitude polar cusp, *Geophys. Res. Lett, 9*, 921-924, 1982.

Carlson, C. W., and R. B. Torbert, Solar wind ion injections in the morning auroral oval, *J. Geophys. Res., 85*, 2903-2908, 1980.

Clauer, C. R., and P. M. Banks, Relationship of the interplanetary electric field to the high-latitude ionospheric electric field and currents: Observations and model simulation, *J. Geophys. Res., 91*, 6959-6971, 1986.

Clemmons, J. H., C. W. Carlson, and M. H. Boehm, Impulsive ion injections in the morning auroral region, *J. Geophys. Res., 100*, 12,133-12,149, 1995.

Elphinstone, R. D., K. Jankowska, J. S. Murphree, and L. L. Cogger, The configuration of the auroral distribution for interplanetary magnetic field Bz northward, 1, IMF Bx and By dependence as observed by Viking satellite, *J.*

Geophys. Res., 95, 5791-5804, 1990.

Friis-Christensen, E., and J. Wilhjelm, Polar cap currents for different directions of the interplanetary magnetic field in the *Y-Z* plane, *J. Geophys. Res., 80*, 1248-1260, 1975.

Knipp, D. J., A. D. Richmond, B. Emery, N. U. Crooker, O. de la Beaujardiere, D. Evans, and H. Kroehl, Ionospheric convection response to changing IMF direction, *Geophys. Res. Lett., 18*, 721-724, 1991.

Lemaire, J., Impulsive penetration of filamentary plasma elements into the magnetospheres of the Earth and Jupiter, *Planet. Space Sci.*, *25*, 887-890, 1977.

Matsuura, N., Mechanisms on the solar wind-magnetosphere interactions: Importance of the Svalbard radar, *J. Geomagn. Geoelectr., 47*, 721-733, 1995.

Maynard, N. C., T. L. Aggson, E. M. Basinska, W. J. Burke, P. Craven, W. K. Peterson, M. Sugiura, and D. R. Weimer, Magnetospheric boundary dynamics: DE 1 and DE 2 observations near the magnetopause and cusp, *J. Geophys. Res., 96*, 3505-3522, 1991.

McDiarmid, I. B., J. R. Burrows, and M. D. Wilson, Large-scale magnetic field perturbations and particle measurements at 1400 km on the dayside, *J. Geophys. Res., 84*, 1431-1441, 1979.

Newell, P. T., and C.-I. Meng, Cusp width and *Bz*: Observations and a conceptual model, *J. Geophys. Res., 92*, 13,673-13,678, 1987.

Newell, P. T., and C.-I. Meng, Ionospheric projections of magnetospheric regions under low and high solar wind pressure conditions, *J. Geophys. Res.*, *99*, 273-286, 1994.

Nilsson, H., M. Yamauchi, L. Eliasson, O. Norberg, and J. Clemmons, Ionospheric signature of the cusp as seen by incoherent scatter radar, *J. Geophys. Res., 101*, 10,947-10,963, 1996.

Norberg, O., M. Yamauchi, L. Eliasson, and R. Lundin, Freja observations of multiple injection events in the cusp, *Geophys. Res. Lett.*, *21*, 1919-1922, 1994.

Petrinec et al., Geomagnetic sudden commencement on February 21, 1994, I, S*TEP GBRSC News, 5,* no. 1, 1995.

Rees, M. H., *Physics and Chemistry of the Upper Atmosphere*, Cambridge Univ. Press, New York, 1989.

Reiff, P. H., T. W. Hill, and J. L. Burch, Solar wind plasma injection at the dayside magnetospheric cusp, *J. Geophys. Res., 82*, 479-491, 1977.

Roble, R. G., and M. H. Rees, Time-dependent studies of the aurora: effects of particle precipitation on the dynamic morphology of ionospheric and atmospheric properties, *Planet. Space Sci., 25*, 991-1010, 1977.

Sandholt, P. E., et al., Cusp/cleft auroral activity in relation to solar wind dynamic pressure, interplanetary magnetic field *Bz* and *By*, *J. Geophys. Res., 99*, 17,323-17,342, 1994.

Stasiewicz, K., A global model of gyroviscous field lines merging at the

magnetopause, *J. Geophys. Res., 96*, 77-86, 1991.

Watermann, J., D. Lummerzheim, O. de la Beaujardiere, P. T. Newell, and F. J. Rich, Ionospheric footprint of magnetosheath-like particle precipitation, *J. Geophys. Res., 99*, 3855-3867, 1994.

Woch, J., and R. Lundin, Magnetosheath plasma precipitation in the polar cusp and its control by the interplanetary magnetic field, *J. Geophys. Res., 97*, 1421-1430, 1992a.

Woch, J., and R. Lundin, Signature of transient boundary layer processes observed with Viking, *J. Geophys. Res., 97*, 1431-1447, 1992b.

Woch, J., and R. Lundin, The low-latitude boundary layer at midaltitudes: Identification based on Viking hot plasma data, *Geophys. Res. Lett., 20*, 979-982, 1993.

Yamauchi, M., and T. Araki, The interplanetary magnetic field B_Y-dependent field-aligned current in the dayside polar cap under quiet conditions, *J. Geophys. Res., 94*, 2684-2690, 1989.

Yamauchi, M., and R. Lundin, Classification of large-scale and meso-scale ion dispersion patterns observed by Viking over the cusp-mantle region, in *Physical Signatures of Magnetospheric Boundary Layer Process*, edited by J. A. Holtet and A. Egeland, pp. 99-109, Kluwer Acad. Norwell, Mass. 1994.

Yamauchi, M., R. Lundin, and T. A. Potemra, Dynamic response of the cusp morphology to the interplanetary magnetic field changes: An example observed by Viking, *J. Geophys. Res., 100*, 7661-7670, 1995.

L. Blomberg, Institute of Plasma Physics, Royal Institute of Technology, S-10044 Stockholm, Sweden. (e-mail: blomberg@plasma.kth.se)

M. Boehm,, MS 169-506, JPL, 4800 Oak Grove Drive, Pasadena, CA 91109. (e-mail: mboehm@jplsp.jpl.nasa.gov)

J. Clemmons and R. P. Lepping, NASA Goddard Space Flight Center, Greenbelt, MD 20771. (e-mail: Jim.Clemmons@gsfc.nasa.gov, RPL@leprpl.gsfc.nasa.gov)

L. Eliasson, H. Nilsson, O. Norberg, and M. Yamauchi, Swedish Institute of Space Physics, Box 812, S-98128 Kiruna, Sweden. (e-mail: lars, hane, olle, yama@irf.se)

S. Kokubun, STE-Lab, Nagoya University, 3-13 Honohara, Toyokawa, Aichi 442, Japan. (e-mail: kokubun@stelab.nagoya-u.ac.jp)

T. Mukai and T. Yamamoto, ISAS, 3-1-1 Yoshinodai, Sagamihara, Kanagawa 229, Japan. (e-mail: mukai, yamamoto@gtl.isas.ac.jp)

S.-I. Ohtani, APL/JHU, Laurel, MD 20723-6099. (e-mail: ohtani@jhuapl.edu)

T. Terasawa, Department of Earth and Planetary Physics, Tokyo University, 7-3-1 Hongo, Bunkyo, Tokyo 113, Japan. (e-mail: terasawa@grl.s.u-tokyo.ac.jp)

(Received January 11, 1996; revised May 6, 1996;

accepted June 10, 1996.)

Paper number 96JA01873.
0148-0227/96/96JA-01873$09.00

YAMAUCHI ET AL.: CUSP DURING INTENSE CORONAL MASS EJECTION
YAMAUCHI ET AL.: CUSP DURING INTENSE CORONAL MASS EJECTION
YAMAUCHI ET AL.: CUSP DURING INTENSE CORONAL MASS EJECTION
YAMAUCHI ET AL.: CUSP DURING INTENSE CORONAL MASS EJECTION
YAMAUCHI ET AL.: CUSP DURING INTENSE CORONAL MASS EJECTION
YAMAUCHI ET AL.: CUSP DURING INTENSE CORONAL MASS EJECTION
YAMAUCHI ET AL.: CUSP DURING INTENSE CORONAL MASS EJECTION
YAMAUCHI ET AL.: CUSP DURING INTENSE CORONAL MASS EJECTION
YAMAUCHI ET AL.: CUSP DURING INTENSE CORONAL MASS EJECTION
YAMAUCHI ET AL.: CUSP DURING INTENSE CORONAL MASS EJECTION
YAMAUCHI ET AL.: CUSP DURING INTENSE CORONAL MASS EJECTION
YAMAUCHI ET AL.: CUSP DURING INTENSE CORONAL MASS EJECTION
YAMAUCHI ET AL.: CUSP DURING INTENSE CORONAL MASS EJECTION

Figure Captions

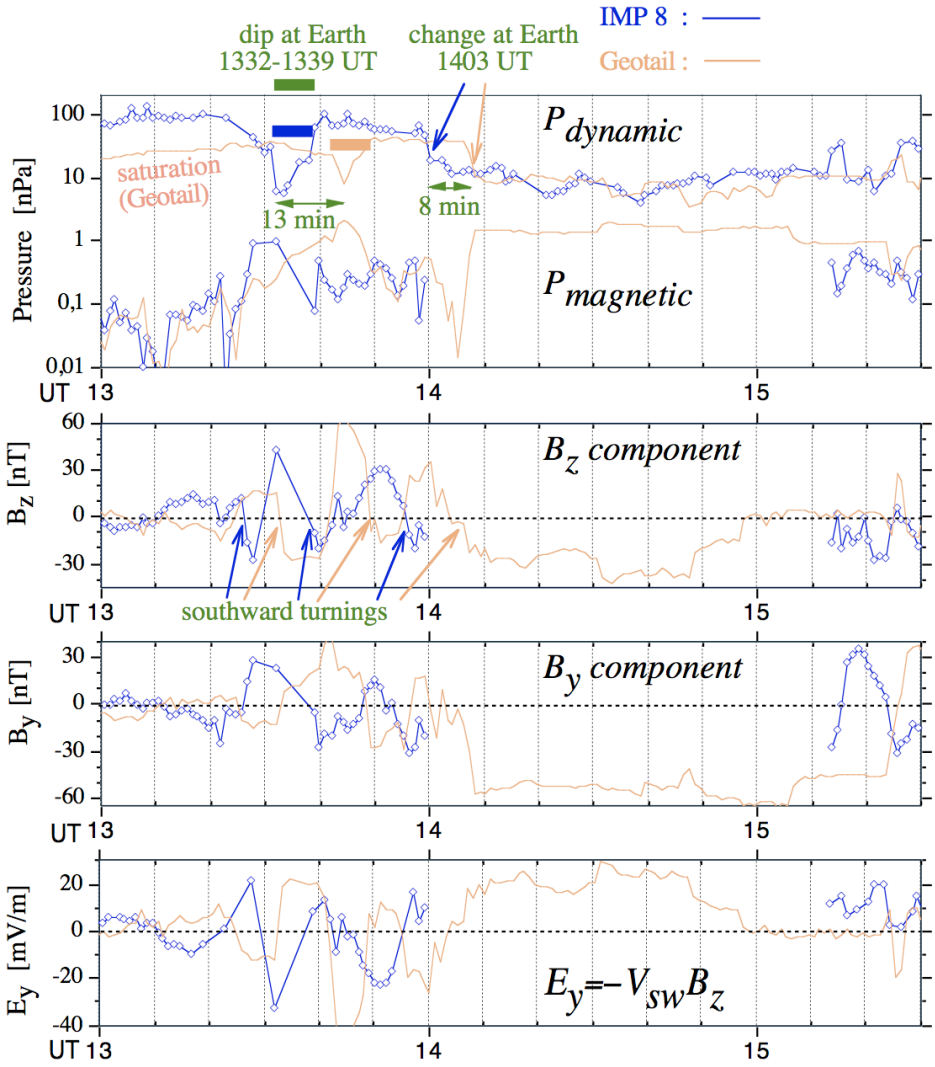

Figure 1. Solar wind parameters in GSE coordinate for 0800 - 2400 UT on February 21, 1994, measured by IMP 8 (dark lines) and Geotail (light lines). The solar wind density (N_{SW}) and velocity (V_{SW}) are shown with a logarithmic scale, and the interplanetary magnetic (B) and electric field (E) are shown with a linear scale. Geotail sometimes (1100-1400 UT) registered much lower-density values than IMP 8 because of the saturation of the sensor. The saturation level is affected by the plasma temperature and is not constant. The IMF condition at Earth is unclear at 1800 - 1930 UT (indicated by dashed hatch which includes orbit 6654) because two satellite registered quite different values; except this period both satellites show the same profile, indicating that the variations in the solar wind belong to large-scale structures. Since the velocity is very steady (at about 800 km/s), the dynamic pressure reflects the density profile. Thin dashed lines indicate the Freja cusp traversals (expected times to cross over the cusp). Orbit numbers are listed at the bottom together with the cusp location in corrected geomagnetic latitude (orbits without the cusp signatures are written inside parentheses). Since Freja was traversing nearly along the same latitude over the dayside, we can determine the lowest possible latitude of the cusp on

orbits 6654 and 6655 (IMF B_Y effect is taken into account for this.) Søndre Strømfjord radar was operated during the indicated period.

Figure 2. Locations of the IMP 8 and Geotail satellites in the GSM coordinates. Since the solar wind velocity is nearly constant (800 km/s), the expected time gap between the two satellites for a radial structure (no dawn-dusk dependence) in the solar wind should be 8 min (25+35 = 60 R_E distance), and it is expected to arrive at Earth 4 min after arriving at IMP 8. If the structure is aligned along the 45° inclined sector boundary, the expected time gap is 3 min (60-37 = 23 R_E distance), and arrival delay to the Earth will be 6-7 min. For the opposite case (longer time gap than 10 min) the arrival at Earth is nearly simultaneous with arrival at IMP 8. All these estimations assume that the shape of the structure is straight.

Figure 3. Data from Freja ion spectrometer, TICS, and electron spectrometers, MATE and TESP, for orbit 6651. TICS measures 1 eV - 4.5 keV positive ions in 0.4 sec (10 ms per each energy). A magnetic deflection system is used to determine the mass/charge ratio, and the instrument easily distinguishes between oxygen ions and protons (top two panels). MATE measures the total number of 2-300 keV electrons from 2π direction every 10 ms. TESP obtains a 20 eV-25 keV electron-spectrum every 32 ms (1 ms per each energy). (a) Overall spectrogram for 90° ± 10° pitch angles between 1317:20 - 1330:20 UT. (b) Blow up of one of the "multiple injections" with full pitch angle coverage between 1323:00 - 1325:00 UT. Overlapping injections are apparent.

Figure 4. Same as Figure 3, except for orbit 6652 for 1506:00 - 1524:00 UT.

Figure 5. Freja (a) magnetic field and (b) electric field observations at orbit 6652 on February 21, 1994. The electric field measurement is in the dawn-dusk direction, and positive values in the electric field correspond to antisunward convection. The baseline for the electric field (heavy solid line) is estimated from the large-scale magnetic field measurement (zero electric field corresponds to zero magnetic deviation in large scale.)

Figure 6. Latitudinal scan plots of the ionospheric parameters (electron density, electron and ion temperatures, and ion drift velocity) obtained by the Søndre Strømfjord radar on February 21, 1994. The radar's field of view is 69° to 74° corrected geomagnetic latitude (CGL). The UT and magnetic local time (MLT) difference is about 2 hours (1400 UT is about 12 MLT). The basic time resolution (each radar beam) is 10 s, and one scan cycle is about 3 min. The scan directions (north-south or south-north) are indicated by the arrows. Drift velocity (line-of-sight direction) is positive away from the radar. Details are described in *Nilsson et al.* [1996].

Figure 7. Solar wind parameters for 1300 - 1430 UT on February 21, 1994, measured by IMP 8 satellite (dark lines) and Geotail satellite (light lines). (top to bottom) Dynamic and magnetic pressure with a logarithmic scale; IMF southward component; IMF duskward component; and interplanetary electric field duskward component. From the time lag between two satellites the arrival times of the changes at the Earth can be estimated with linear interpolation (see Figure 2): They are 1332 and 1403 UT for SWDP or dynamic b, 1517 UT for B_Y, and 1330, 1343, and 1401 UT for IMF B_Z (and E_Y).

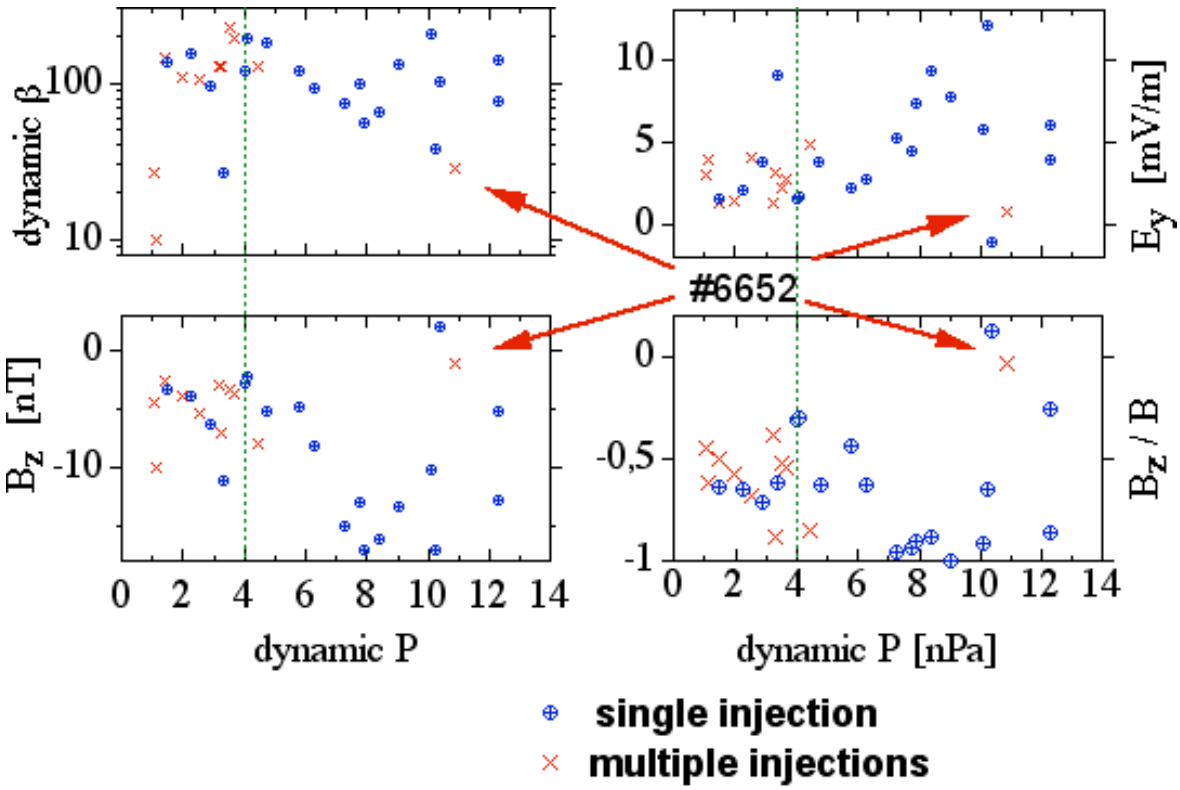

Figure 8. Observations of clear single-injections and clear multiple injections plotted as functions of dynamic pressure and the other solar wind parameters (IMF B_Z, $B_Z/|B|$, and $E_Y = -V_{SW}B_Z$). All Freja cusp observation from November 1992 to May 1995 are used. Note that *Newell and Meng* [1994] used the threshold for high and low SWDP as above 4 nPa and below 2 nPa, respectively. Multiple injections with one injection detected and the others undetected are eliminated by taking only intense and long (more than 1 min of cusp detection) cases. Since we do not find any intensity-dependence of the cusp morphology (not shown here), most of the "single-injection" examples at moderate pressure (< 4.5 nPa; left of the dotted line) must be the real single-injection cases.

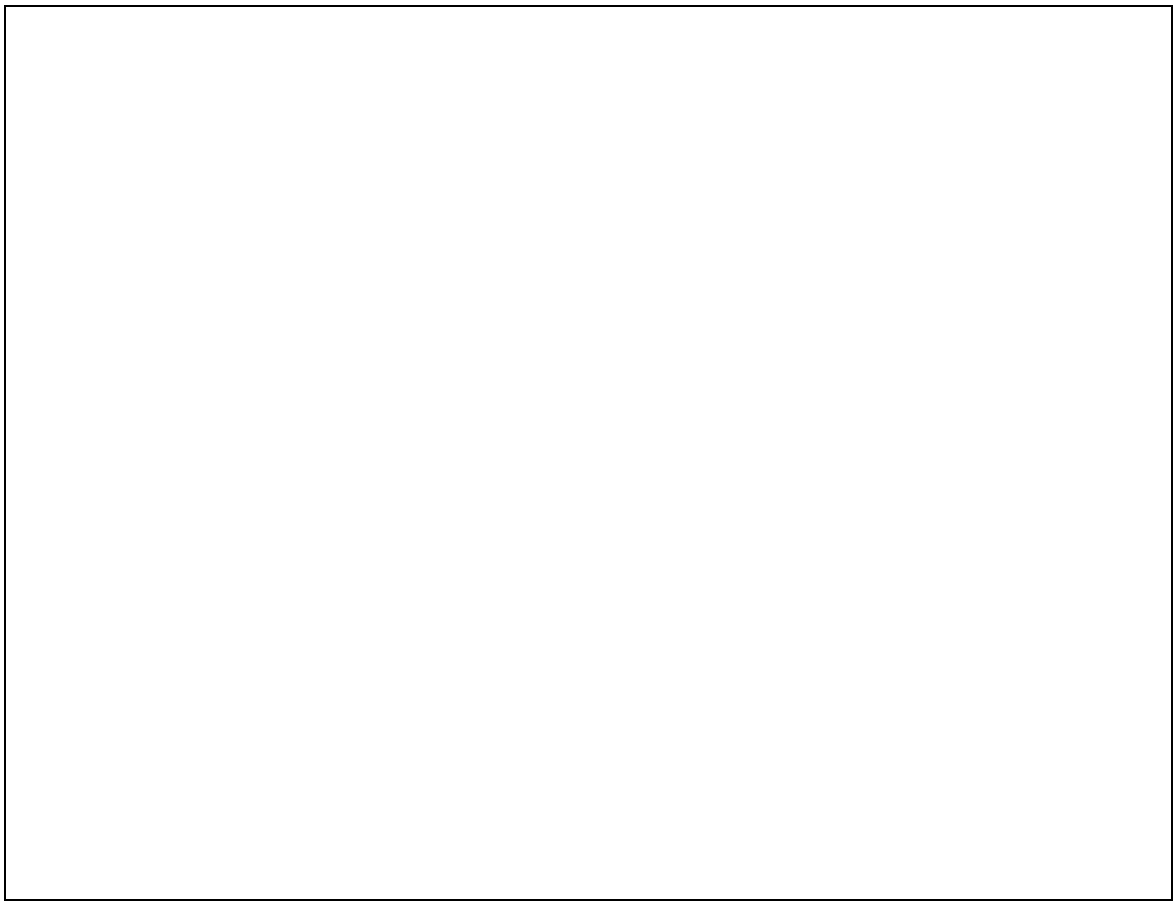

Plate 1. Overall plot (time versus latitude) of electron density observed by Søndre Strømfjord radar. This is constructed from Figure 6. Freja trajectories are superposed on the figure. Freja orbit 6651 (cf. Figure 3): The indicated part of the orbit covers 1328 - 1330 UT, when Freja observed weak magnetosheath-like precipitation, separated from a very strong magnetosheath-like particle precipitation event observed between 1326 and 1327 UT. Freja orbit 6652 (cf. Figure 4): Weak magnetosheath-like precipitation appears at around 13.5 MLT. The electron temperature enhancements in these radar scans are not very high, but the sudden appearance of an electron density enhancement at 1526 UT, which is seen also at low altitudes, gives evidence of precipitation. Very high ion temperatures are also seen.

§ Oxygen injection event at dayside (February 21 1994)

At the first conjugate point, Freja observed a weak and isolated ion precipitation at 70.0-70.8 CGLAT, which is separated only 250 km from the most intense particle precipitation region at 1327 UT (even O^+ are seen). The energy of the oxygen (1 keV) is lower than that of proton (> 3 keV) where they are overlapped. Probably the oxygens are cold magnetospheric one, which simply mixed with the injecting magnetosheath plasma and is dragged by that bulk flow when they are mixed (mixing must be asymmetric; i.e., it is NOT the traditional reconnection type on the de-Hoffman frame.) If the locational separation of the O^+ and protons were simply due the time of flight effect, we must see an ion dispersion, but the data does not show it. The same difficulty arises if the locational separation is caused by the velocity filter. A possible interpretation is that the convection direction of proton and that of oxygen are different and independent each other. This breaks down the MHD treatment for the mixing mechanism of the magnetosheath proton and magnetospheric ion.

For example, we see two unusual particle injections near local noon. (1) Heavy ion injection (0.5-1 keV) is observed at 13 MLT (1331:30 UT) during the first pass (orbit 6651). The injection is immediately followed by proton (10-30 eV). The oxygen is much faster than the proton in velocity if we take the same UT. The injection location of 13 MLT is quite unusual (only a few case among out of nearly a thousand of Freja dayside traversals), and presently we have no explanation on this phenomenon. The heavy ion injection observed by Freja at all local time will be reported in a separated paper. (2) A less intense plasma injection is observed equatorward of the cusp (1329 UT in Figure 3a). This is similar to the stagnant plasma injection (SPI) event [Yamauchi et al, 1993]. The SPI event is often observed by Viking satellite but very rarely found by Freja. So, this observation is also unusual.